



Exploring Wake Interactions in a Counterrotating Dual Rotor System for different Yaw configurations: An Experimental Study

Jannis Maus^{1,2}, Joachim Peinke^{1,2}, and Michael Hölling^{1,2}

¹Carl von Ossietzky Universität Oldenburg, School of Mathematics and Science, Institute of Physics

²ForWind - Center for Wind Energy Research, Kükpersweg 70, 26129 Oldenburg, Germany

Correspondence: Jannis Maus (jannis.maus@uni-oldenburg.de)

Abstract.

As an opportunity to increase turbine and wind park efficiencies, multi and dual rotor turbines have received great attention among research and industry. Goal of this experimental study is to validate and add findings to numerical simulations on dual rotors. It will be shown that the rotational sense greatly influences the lateral interaction and hence the downstream evolution of a dual wake. In the experiments, 19 hot-wires on a downstream traversing array are used to acquire the velocities in the wake at high temporal and spatial resolution. Two laterally spaced counterrotating model wind turbines with a diameter of 0.58 m (= 1 D) generate the wake, which is analyzed between 0.75 - 10.0 D downstream. The benefits in dual rotor wake control will be shown through symmetrical yaw-alternation of the setup in dependency of the positioning of the turbines with different rotational sense. To achieve a beneficial wake evolution for a downwind turbine, two main strategies are presented. One is a wake centroid deflection away from a possible downstream turbine, causing a flow entrainment from above the dual rotor setup. The other one is an induced wake collision, resulting in strong turbulent interaction between the two single wakes and faster wake recovery. The knowledge of these principles and their application to full scale show great potential for large efficiency gains in terms of wind park operation.

1 Introduction

With electricity generation being the strongest emitter of greenhouse gas emission, it is the duty of the renewable energy sectors to substitute fossil fuels and cope with the ever increasing world wide electricity demand (Newell et al. (2019); Ge and Friedrich (2020)). Especially wind farms and their optimizations have received great attention in this process. Aiming for a maximization of power output per area, it is being explored how to arrange and control these wind farms, while considering economical, environmental, technical or social variables. Following, the global trend shows ever increasing rotor diameters and multi megawatt rated turbines at and above 15 MW, which are being tested and installed offshore. But not only larger turbines are being considered. Within this transition, many researchers have put attention to the substitution of traditional three-bladed wind power plants with so-called multi-rotor turbines. This emerging technology does not only promise lower maintenance- or construction-costs, especially the promoted positive effect on the wake recovery and an increase in power generation show great potential for large scale usage (Ghaisas et al. (2020); Bastankhah and Porté-Agel (2019); Chasapogiannis et al. (2014);



25 Van Der Laan and Abkar (2019); Sandhu and Chanana (2018)). In order to capitalize from these promising effects, leading companies like EnBW or Vestas implemented first scaled prototypes with two or four rotors in the German baltic sea (EnBW and Aerodyn (2021); Van Der Laan and Abkar (2019)). In fact, the Chinese company Ming Yang Smart Energy deployed the worlds largest floating turbine (16.6 MW) as a dual rotor in 2024 and announced plans for an ultra-large 50 MW dual rotor in late 2025 (Memija (2025)), showcasing the immense potential of this technology.

30 In terms of wind farm optimization, especially the wake recovery behind the closely spaced rotors is of great interest. Various studies present different numeric modeling approaches on double or multi rotor wakes, focusing on wake mixing and its consequence for the wind velocity development in horizontal and vertical dimensions. A comprehensive large-eddy-simulation by Bastankhah and Porté-Agel (2019) introduced first insights to the wake interaction behind a closely spaced multi-rotor with four turbines in comparison to a single rotor with the same rated power. The simulations showed a better wake recovery, hence
35 lower values of velocity deficit and turbulence intensity at downstream locations. Whilst maintaining the same setup of a four-turbine multi-rotor, Speakman et al. (2021) follows up with an investigation on the impact of yaw on the wake. The investigated setups use so-called coning or channeling to divert or focus the multi-rotor wake in the desired way. Their simulations suggest that especially the ease in controllability of the rotor wake and the magnitude and distribution of the velocity deficit show great potential to improve wind park efficiency. Addressing the increasing amount of implemented or planned full-scale prototypes,
40 Mendoza et al. (2023) focus on the wake and the aerodynamic performance of a dual rotor concept in a uniform inflow. In accordance with previous multi-rotor simulations, also the dual rotor provides a higher power output per turbine compared to a stand alone single-tower setup. Especially below rated wind speed a significant increase in power generation and wake recovery can be identified (Mendoza et al. (2023); Maus et al. (2022)).

Although numerical simulations and models have achieved broad acceptance and are highly precise in replicating both large
45 and small scale phenomena, experimental validation helps to assure all processes happening in the turbulent mixture of two wakes. For instance, Wu and Porté-Agel (2011) already declared in the application of the widely used rotating actuator disk model, used in the simulations of Bastankhah and Porté-Agel (2019) and Speakman et al. (2021) that the wake rotation in the simulation proved to be underrepresented, when compared to actual measurements in the wind tunnel.

Therefore, this experimental study shall help to not only validate the simulations of a dual rotor concept, but clarify mechanisms
50 of the wake formation and the lateral interaction of the individual wakes. This will be achieved experimentally through a systematic variation of rotational sense and yaw displacement in the setup after having varied the lateral spacing beforehand (Maus et al. (2022)). The velocity deficit u_{Def} , the turbulent kinetic energy $\langle u'^2 \rangle$, the recovery rate Z and the relative wind velocity U_{Rel} in the downstream wake shall give a sound overview on the relevant aspects of the dual rotor wake recovery.

2 Methodology

55 2.1 Experimental Setup

The measurements were conducted in a Göttingen type wind tunnel with a test section size of $3 \times 3 \times 30 \text{ m}^3$. Temperature, ambient pressure and relative humidity were constantly monitored and accounted for when calibrating the measurement devices



and executing the experiments.

The wake was measured by 19 horizontally spaced hot-wires mounted at hub height on a traversing system, allowing for easy and precise velocity measurements in the wake. Additionally, a *Prandtl Tube* was mounted 2.5 D above the measurement plane acquiring the reference speed of the undisturbed inflow (see Figure 1).

Two MoWiTO 0.6 (**Model Wind Turbine Oldenburg**) with a diameter of 0.58 m served as wake generators. Through utilization of low-Reynolds airfoils, similar power coefficients to a full scale turbine can be achieved (Schottler et al. (2016, 2018)). The turbine is mainly operated by a collective pitch mechanism and a proportional-integral-derivative (PID) controller allowing for an automated generator torque control. An upfront calibration of the PID controller allows for an automated operation even in turbulent inflow conditions in the partial load region of the turbine (Schottler (2018)).

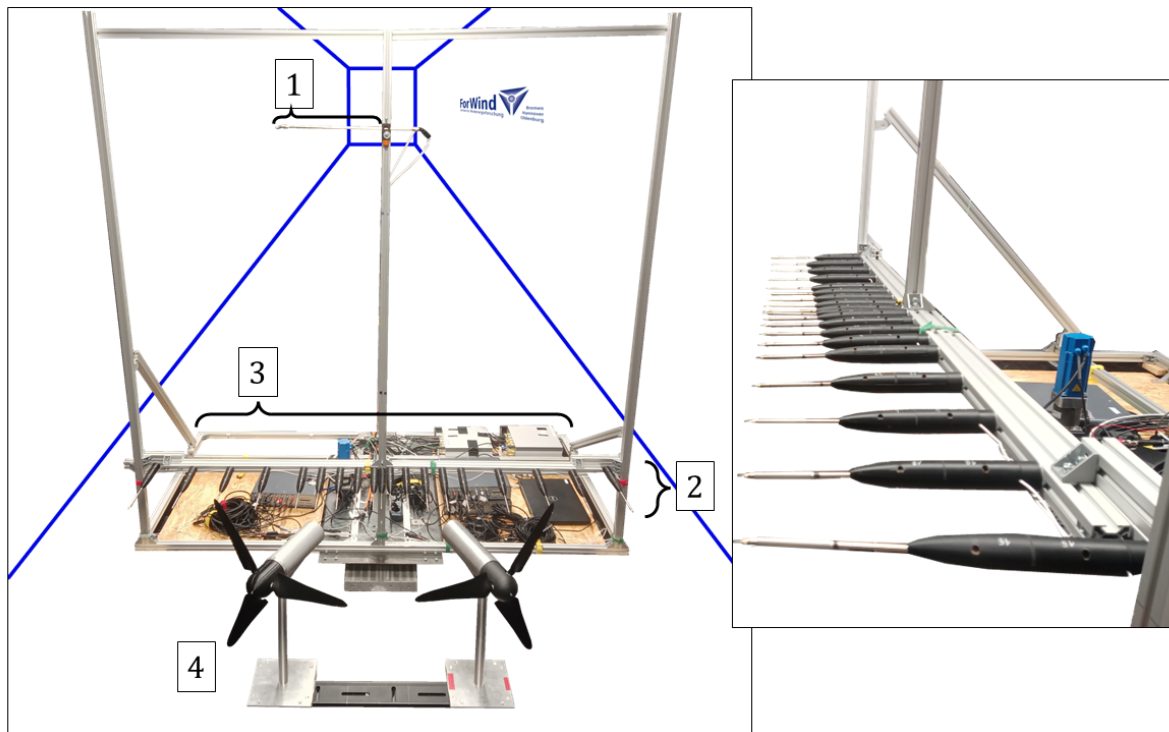


Figure 1. *Left:* Experimental setup including (1) a Prandtl Tube, (2) hot-wires, (3) AD-converters, power-supply and Mini-CTAs together with (4) two MoWiTO 0.6 in a yawed configuration. *Right:* Hot-wire probes at hub-height in an aerodynamically optimized mount.

One of the turbines is equipped with clockwise rotating blades (dyed in blue in the following figures), the other one with counter-clockwise rotating blades (dyed in red in the following figures). Hence, two major setups will be realized and analyzed in this study: one configuration with the counter-clockwise rotating turbine right of the clockwise rotating turbine, further referred to as "Counter-Right" (CR), and a second configuration with the counter clockwise rotating turbine on the left, further referred to as "Counter-Left" (CL). While different studies by Schottler et al. (2016), Neunaber et al. (2020) or Messmer et al.



(2022) have already dealt with and proven the validity of these model-turbine wakes and their comparability to full scale turbine wakes, subsection 3.1 Single Rotor Wake gives more insight to the parametrization of the individual MoWiTO 0.6 wake.

2.2 Experimental Procedure

75 In preliminary measurements (Maus et al. (2022)) it was found that the wake recovery in laminar inflow of the model wind turbine does not change greatly among different wind speeds. Therefore all measurements were taken at a laminar inflow velocity of 5 ms^{-1} , corresponding to the partial load region of the turbine. The hot-wire measurements were taken between $0.75 - 10.0 D$ downstream of the turbine, while D refers to the turbine diameter of 0.58 m . All lateral and downstream measurement positions can be seen in Figure 2, with the highest spacial resolution along the centerline. In order to achieve a statistically meaningful number of measurements, the total recording time was set at 240 seconds at a sampling frequency of 6 kHz , with a low-pass filtering at 3 kHz .

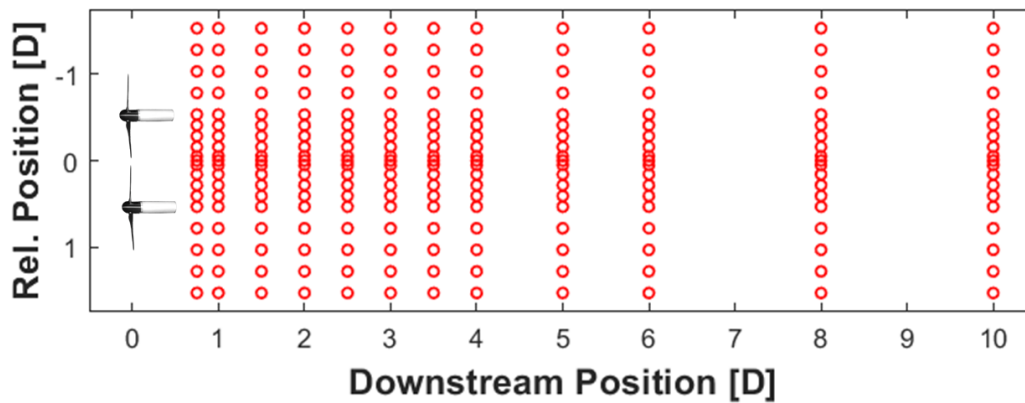


Figure 2. Measurement points along the downstream wake of the dual rotor..

First of all, both the clockwise and counter-clockwise rotating turbine were analyzed individually in the given setup. This means that only one turbine at a time is placed in the wind tunnel, starting with 0° yaw displacement and then altering between 20° , 15° , 10° and 5° yaw to the left and to the right, so that in total 9 different configurations were realized per turbine.

85 In the dual rotor system, the lateral distance between the two turbines was chosen to be $1.07 D$ for a number of reasons. Previous investigations on the lateral spacing between the turbines showed highest wake-wake interaction below a lateral spacing of $1.15 D$ (Maus et al. (2022)). The closer the turbines were moved together, the more power output of the dual rotor system was monitored, however a safety margin of $0.07 D$ ($\hat{=} 4 \text{ cm}$) had to be maintained to avoid tip collision. Finally, also other numerical studies use similar hub distances between $1.05 - 1.10 D$ for a dual- or multi-rotor setup (Speakman et al. (2021); Chasapogiannis et al. (2014); Mendoza et al. (2023)).

The different yaw configurations of the two dual-rotor setups Counter-Left and Counter-Right were achieved through the following procedure. After the reference case of 0° , the turbines were yawed symmetrically either inwards or outwards at 5° ,



10°, 15° and 20°, so that 9 different alignments were analyzed per rotational configuration (CL or CR) .

Following parameters were derived from the data: the normalized wind speed deficit u_{Def} , the turbulent kinetic energy TKE ,
95 the wake recovery rate Z and the relative wind velocity in the wake U_{Rel} :

$$u_{Def} = 1 - \left(\frac{\langle u \rangle}{u_0} \right) \quad (1)$$

$$TKE = \langle u'^2 \rangle \quad \text{with } u' = u(t) - \langle u \rangle \quad (2)$$

$$100 \quad Z = \left(\frac{\langle u_{x_1, y_1} \rangle - \langle u_{x_2, y_1} \rangle}{x_2 - x_1} \right) \quad (3)$$

$$U_{Rel} = \frac{U_{Wake}}{U_{Ref}} \quad (4)$$

$$\text{with } U_{Wake} = \int_{-1.035}^{1.035} \langle u(y) \rangle dy. \quad (5)$$

105

$\langle u \rangle$ refers to the mean velocity of each hot-wire, u_0 refers to the reference inflow wind speed in the wind tunnel, $u(t)$ is the measurement time series and u_{x_1, y_1} and u_{x_2, y_1} are two wind speeds at same lateral, but different downwind position. U_{Rel} is the ratio between the average wind speed in the wake (U_{Wake}) and the reference wind speed (U_{Ref}), calculated through the
110 integral of the mean wind velocities over the dual rotor turbine span from -1.035 to +1.035 D, hence in y-direction.

3 Results

The following chapters offer a systematic approach on the mechanisms of a dual rotor wake formation and their possible benefits. In order to break down different steps in the evolution of the wakes and characterizing the interaction between the two turbines, both rotors were measured individually at first. Afterwards, both u_{Def} and the TKE of the dual rotor setup will
115 be shown for the different yawed and rotational cases. Finally, the wake recovery and relative wind analysis hint at the most crucial parameters and mechanisms in the dual rotor setup.

To describe the different cases, following nomenclature will be used: When describing any setup, the observers perspective shall be looking downwind on the single- or dual-rotor plane. For instance "yawing the turbines inside" means that both turbines are yawed towards the centerline and a wake drift to the left means that the wake moves away from the centerline towards the
120 left wall of the wind tunnel, i.e. the upper end in the following figures. Additionally, also the rotational sense is described looking on the turbine in downwind direction.



3.1 Single Rotor Wake

In order to develop a better understanding on the interaction of the individual wakes in the double rotor configuration, the wakes of the individual turbines are measured first. This data will be used later to explain findings in the behaviour of dual rotor wakes. Hence both the clockwise and counter-clockwise rotating turbines were placed individually within the wind tunnel and all considered yaw-cases (-20° to $+20^\circ$ at 5° steps) were measured with the setup described in subsection 2.2. A negative sign means a counter-clockwise rotation of the nacelle, and a positive sign means a clockwise rotation of the investigated turbine. As an example for 0° and $\pm 20^\circ$ yaw, the following figures will show 2D surface plots of the normalized wind velocity deficit, calculated through Equation 1. All measurement positions are marked with small black dots.

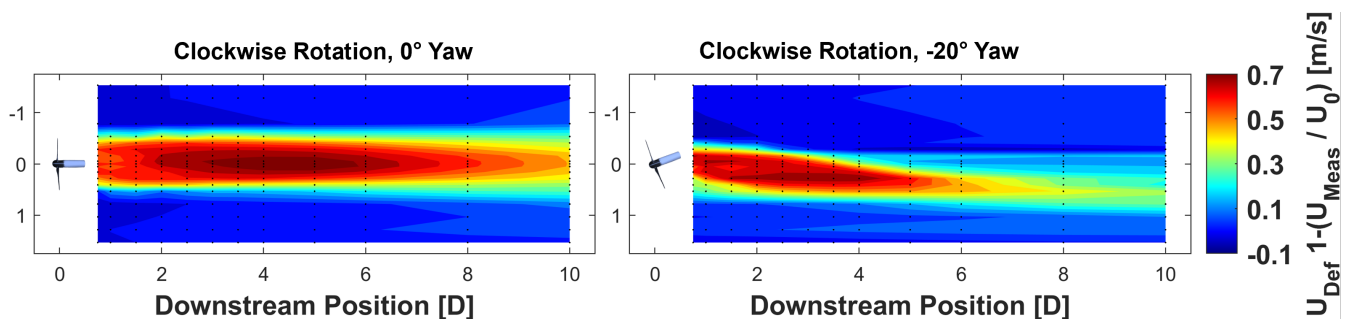


Figure 3. Velocity deficit of a single, clockwise rotating turbine at 0° (left) and -20° yaw (right) rotation.

In accordance to previous studies (Neunaber (2019); Schottler et al. (2018)), the wake of the non-yawed setup (Figure 3) shows the highest velocity deficit between 4-5 D downstream of the rotor plane. At 8-10 D the wake widens and the streamwise velocity along the centroid starts to recover. In contrast, the yawed turbine setup shows the highest velocity deficit between 2-4 D downstream and a better recovery. Additionally, the wake centroid is strongly deflected to the right and it appears that the wake width is not increasing as strong as in the non-yawed case.

The relatively slow recovery of the non-yawed case can be mainly attributed to the laminar inflow of the setup. Previous experimental, numerical and full-scale studies have shown that a low turbulence intensity in the inflow inhibits the entrainment due to an absence of larger turbulent structures and a low lateral kinetic energy flux (Porté-Agel et al. (2020); Cherubini et al. (2022)). Furthermore, visualizations of the setup at hand showed relatively far persisting tip-vortices, preventing necessary shear stress between wake and free flow (Maus (2022)). The obvious wake-center deflection of the yawed rotor can be explained through momentum theory and is a well know mean for wake steering (Jiménez et al. (2010)). The fundamental difference in wake intensity and recovery is partly attributed to the fact that due to yawing the turbine, the projected rotor-area is lowered and the turbine blades are misaligned to the air flow, hence less energy is extracted from the flow. A more detailed view on the wake recovery follows in 3.2.3 Wake Recovery.

For comparison also the individual wakes of the counter-clockwise rotating turbine was investigated at non-yawed and yawed condition.

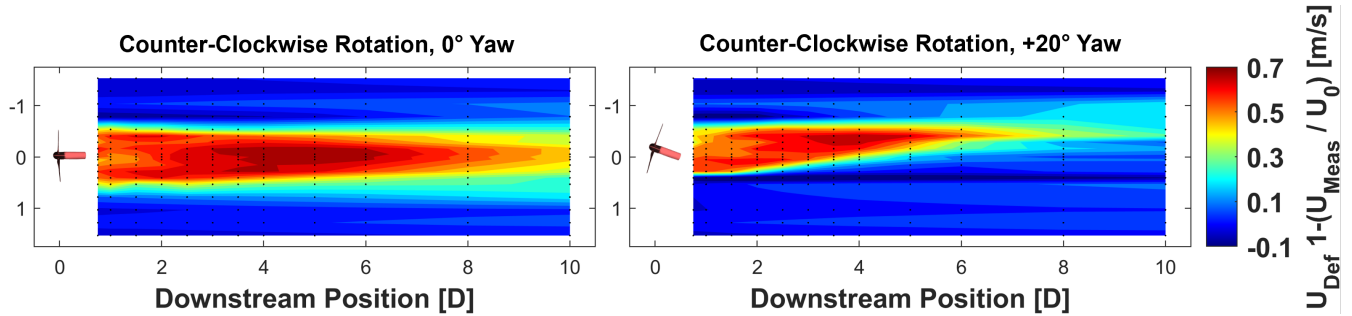


Figure 4. Velocity deficit of single, counter-clockwise rotating turbine at 0° and +20° yaw rotation.

Although the rotational sense of the turbine has changed, the non-yawed wake profile of both turbines have the same main properties: the highest velocity deficit between 4-5 D downstream and a recovering deficit starting after 8-10 D. In order to maintain the comparability, Figure 4 shows the turbine yawing to +20°, which creates a mirror-symmetric picture of the rotor wake towards the clockwise rotating turbine. The wake is deflected to the left and the general recovery is way faster than behind a non-yawed turbine. Maintaining a symmetric initial setup is of high relevance for the comparability of the two turbines (Maus et al. (2022)). In the cases, where the counter-clockwise rotating turbine is yawed in the same direction as the clockwise rotating one, hence breaking the mirror-symmetry, a much wider wake with a higher velocity deficit and a lower wake centroid deflection is measured, as can be seen in the following Figure 5.

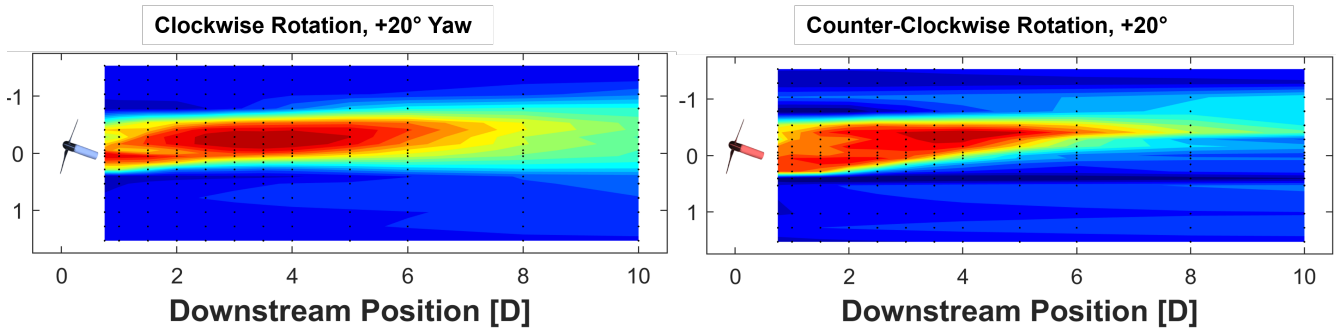


Figure 5. Comparison of single turbine wakes at identical, not mirror-symmetric yaw (+20°).

It can be seen that the wake, especially in yawed condition, widens towards that side, where the tower wake is drawn into the measurement plane. For instance, yawing the clockwise rotating turbine to -20° (Figure 3) causes two advantageous mechanisms: Downstream of the turbine on the right, the wake rotation draws the tower wake to the outside in a beneficial position to mix with the free flow. On the left side, the wake rotates downwards, so that the free flow from above the turbine is entrained into the wake. Both mechanisms benefit the wake recovery, resulting in a lower velocity deficit compared to the non-yawed condition. It can be concluded that the wake of a clockwise rotating turbine can be directed much better to the right and vice



versa for the counter-clockwise rotating turbine. This is especially important when using actuator disks as a substitution for model wind turbines in future wind tunnel investigations. These can achieve very good correlation for thrust-, velocity deficit- or turbulence-values (Howland et al. (2016)). But even though their thinner towers might have a less pronounced effect in the downstream wake evolution, the use of active discs cannot fully account for the important mechanism of wake rotation.

165

3.2 Dual Rotor Wake

3.2.1 Normalized Velocity Deficit

This section will show to what extent the rotational direction and the yaw affect the wake behind a model dual rotor. For reference Figure 6 shows the two dual rotor wakes of CR and CL at a non-yawed configuration. A detailed analysis of this setup was previously described in Maus et al. (2022). It was found that the rotational sense has a significant impact on the wake formation behind the dual rotor. The most prominent effect visible in this plot is the difference in wake width at 10 D behind the rotors. While the CR setup shows nearly no lateral expansion, the wake edges in CL have broadened to about -1.25 to 1.25 D.

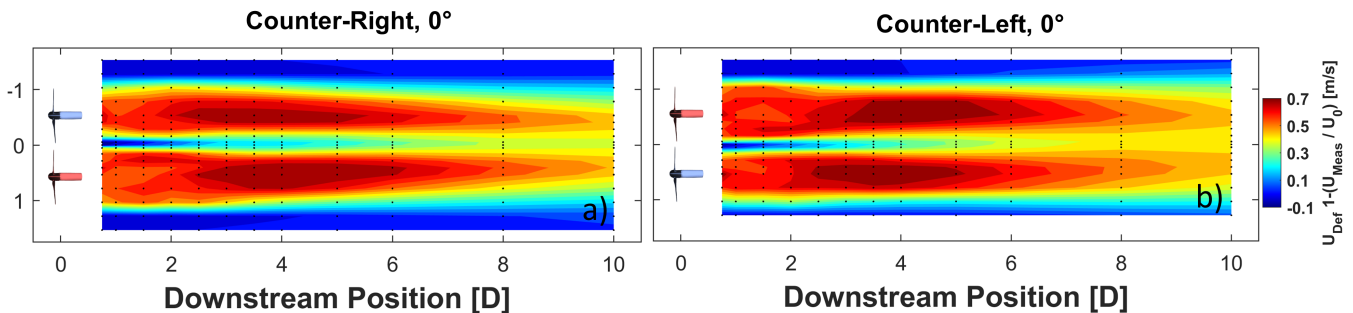


Figure 6. Velocity deficit of both possible rotor configurations at 0° yaw. Counter-clockwise rotating turbine in red and clockwise rotating turbine in blue.

This difference in wake expansion will be promoted to an even greater extent, when looking at yawed configurations of the setups. Figure 7 shows both rotational configurations at 20° inwards and outwards yaw, which are the cases with the strongest yaw displacement investigated in this study.

Even at identical yaw and inflow conditions, the impact of the rotational sense is tremendous. In the CR setup with inwards yaw (Figure 7 a), the two separate wakes merge very quickly into one very narrow wake, which shows a width of less than one turbine diameter at a downstream distance of 6 D. In contrast the same inwards yaw with the counter-clockwise rotating turbine on the left (Figure 7 c) only causes the two rather individual wakes to merge about 4 D behind the rotor, forming a very stable and uniform wake with an approximate width of 2 D, even 10 D downstream.

Yawing both rotors outwards causes a split of the dual rotor wake into two separate individual wakes (Figure 7 b and d).

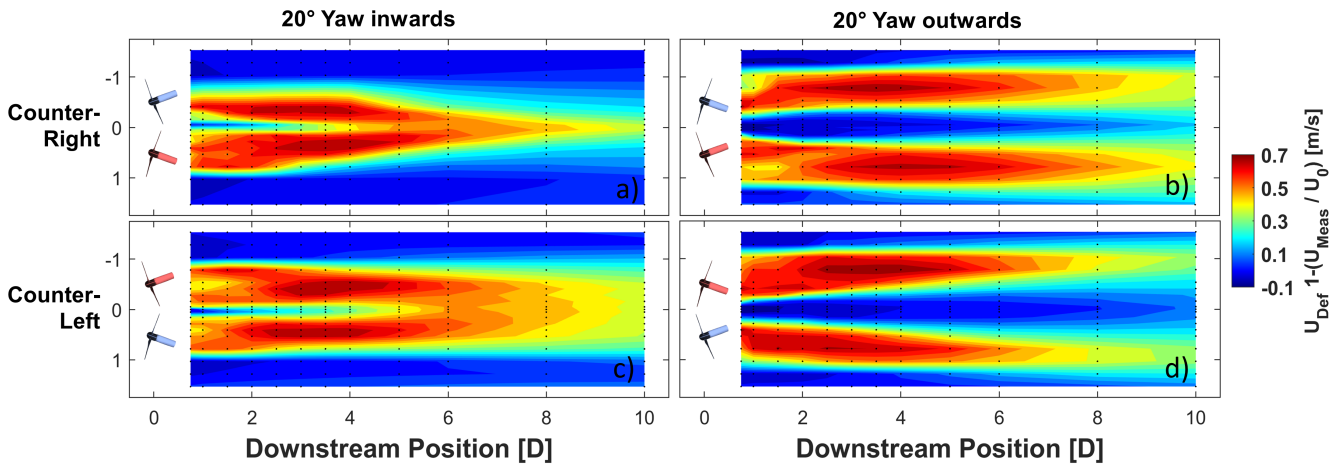


Figure 7. Velocity deficit of both possible rotor configurations at 20° inwards (a and c) and 20° outwards (b and d) yaw. Counter-clockwise rotating turbine in red and clockwise rotating turbine in blue.

Although the wake-similarity of CR and CL for 20° outwards yaw is greater than for the inwards case, a couple of differences can be pointed out. First of all, the single-wake centroids in the CR setup follow a rather straight line in downwind direction. In contrast, the wakes in CL are persistently drifting outwards and the inter-wake space is growing. At 10 D, the wakes in the CR setup meet at the centerline, whereas no wake merging can be observed for CL within the measurement frame. Finally, the normalized velocity deficit of the single wakes in CL have recovered to below 0.5 (orange surface) about 2 D faster than in CR. In the case of CR yawed 20° inwards, the wakes rotate in such a manner that the tower wake is entrained towards the inside of the dual rotor wake. Following, the outer wake edges, which are forced towards the centerline because of the momentum theory, have a large area of interaction with the surrounding free stream, so that uniform flow is entrained into the measurement plane at the wake edges. These mechanisms cause a very narrow residual wake at 8-10 D downstream. In the case of CL yawed 20° outwards the same mechanisms can account for the strong separation of the two individual wakes. Here the undisturbed flow is entrained towards the centerline by the wake rotations of both turbines. For instance, the counter-clockwise rotating turbine with its clockwise rotating wake is pulling the tower wake to the outside of the setup, where the interface between free flow and turbine wake is maximum, resulting in a faster wake decay.

3.2.2 Turbulent Kinetic Energy

In order to validate the theory of the wake rotation drawing the tower wake into the measurement plane, the turbulent kinetic energy can be used to identify added turbulence and highlight important transition regions, which are not visible in the normalized wind speed deficit.

For reference Figure 8 shows both configurations at 0° turbine yaw. Despite only minor differences between the wake width in both setups in Figure 6, the analysis of turbulent kinetic energy reveals stronger differences between the two configurations.

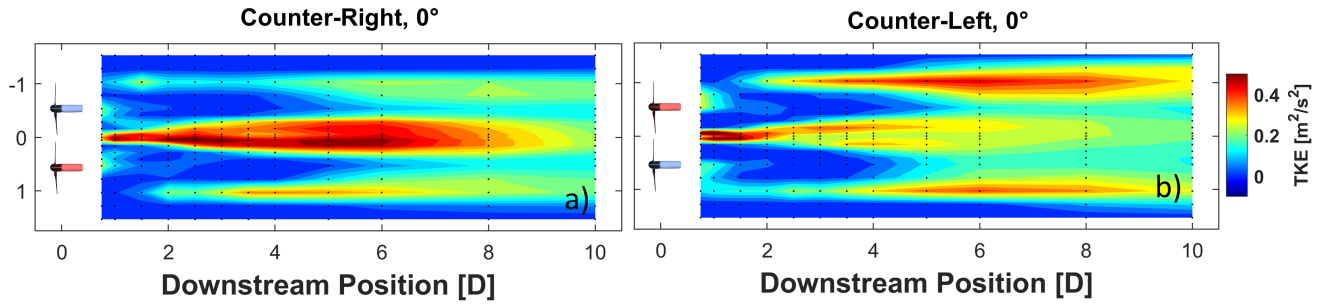


Figure 8. Turbulent kinetic energy of both rotor configurations without yaw. Counter-clockwise rotating turbine in red and clockwise rotating turbine in blue.

While CR (Figure 8 a) shows very high TKE values mostly along the centerline, CL (Figure 8 b) holds multiple smaller areas of increased turbulence levels, spread over the entire measurement plane.

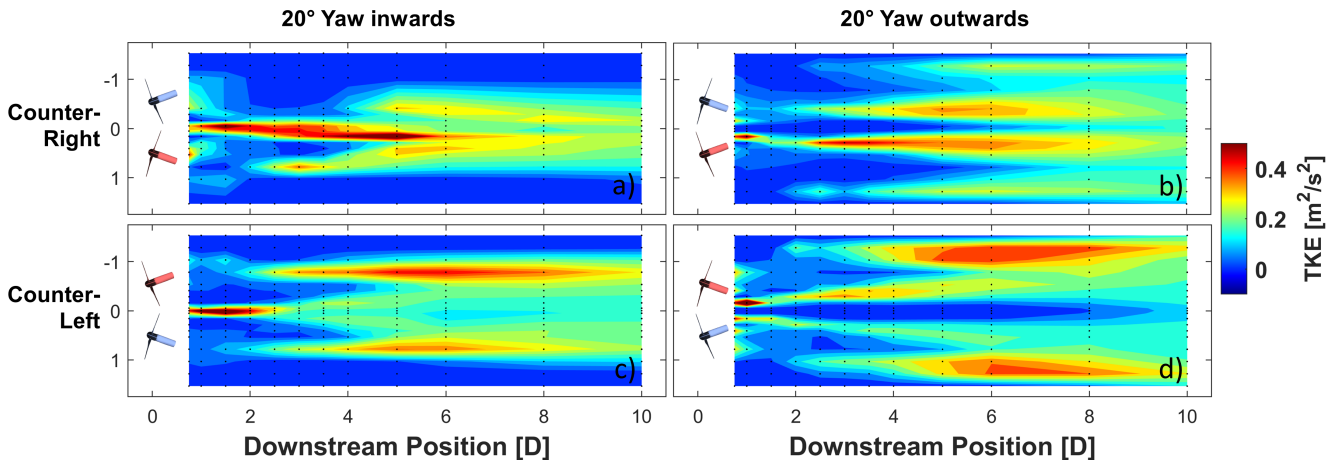


Figure 9. Turbulent kinetic energy of both rotor configurations at 20° inwards (a and c) and 20° outwards (b and d) yaw. Counter-clockwise rotating turbine in red and clockwise rotating turbine in blue.

All center wake fields share the property of a relatively non-turbulent near wake between 1.5-3.5 D downstream of the individual rotors, which shows as dark-to-light blue area in the plot. All other properties however, are very unique for each setup. In Figure 9 (a) with CR at a 20° inwards yaw, the highest TKE -values are found along the centerline of the dual rotor between 1-6 D downstream. CL with a 20° inwards yaw (Figure 9 c) also shows extreme turbulence along the centerline between 1-2.5 D, however then the wake field becomes relatively isotropic, only the outer edges are marked by higher TKE . The turbulence field of the outwards yaw confirms what has been stated before: In Figure 9 (b) the wakes of CR start to interact and mix between 8-10 D downstream, while CL maintains a complete separation not only wind velocity wise, also turbulence wise in Figure 9 (d). Clusters of strongest wind fluctuations are found along the edges of the single wakes between 3-8 D, for



CR especially the inner wake edges and for CL the outer wake edges.

The two main drivers of high turbulence in the MoWiTO 0.6 wake are tip-vortex breakdown and the mixture of tower with rotor wake. In those cases, where both rotors are yawed inwards, the small lateral distance and the deflection of the rotor wakes towards one another cause a very early mixing of the tip vortices. The sudden breakdown shows as a localized area with very high turbulent kinetic energy along the centerline for both CL and CR. While the wake evolves into a relatively homogeneous wake for CL, the high TKE remains for CR. This can be attributed to the fact that after the tip vortices have broken down, the wake has progressed far enough downstream to show the interaction of tower with rotor wake. The rotation has entrained the turbulent structures into the measurement plane and the decay shows as area of high turbulent kinetic energy. In CR and inwards yaw, this shows as a persistently high TKE all the way until 8 D, as the tower wakes of both turbines overlap and mix in this area. In the outwards yaw, the individual wakes have not yet mixed at 4-7 D, but the mixture of tower- and rotor wake can account for the wake widening and mixing further downstream in the outwards yaw setup.

In the two different CL setups, the wake rotation causes the tower shadow and its turbulent decay to show along the outside of the dual rotor wake as an orange stripe. This is the main driver for the strong wake centroid deflection in CL 20° outwards yaw (cf. Figure 7). The entrainment to the inside of the dual rotor helps to keep the wakes separate, or on the inwards yaw case, supports the formation of a relatively large isotropic turbulent field along the centerline of the rotor setup. For completeness it shall be stated that the presented correlations and explanations remain valid for all intermediate setups (5°, 10° and 15° inwards and outwards yaw), however due to the best representation, only the extreme cases with 20° inwards and outwards yaw misalignment are shown here.

3.2.3 Wake Recovery

In order to evaluate the benefit of yawing the turbine-configurations inside or outside, the wake recovery rate Z has been calculated through Equation 3, which mathematically corresponds to the streamwise derivative of the wind speed. A negative value means a deceleration of the flow and a buildup of the wake, and a positive value attributes to the actual decay and recovery of the wake.

It is important to note that Figure 10 shows the overall wake recovery rate in streamwise direction, not lateral or wake centroid direction. Because of the turbine yaw, the wakes are not only evolving in downstream direction, but are deflected sideways, which shows as yellow area in the surface plots.

In general it can be constituted that in the near wake, between 1-3 D downstream of the dual rotor, a lot of mechanisms of wake formation seem to overlay, causing an area with a lot of small patches of both strong recovery or buildup. This can be attributed to the pressure difference trying to balance between free flow and rotor shadow (Boudreau and Dumas (2017)). Further downwind the structures start to form larger patches and the wakes mostly start to recover. Only in Figure 10 (c), a larger dark green area along the centerline between 4-7 D hints at a secondary wake-buildup. Apparently, this is where the collision of the two individual wakes and mixing of their tip vortices causes a further deceleration of the flow, unusually far behind the rotor plane.

The two cases with the most outstanding wake recovery rate are CR at 20° inwards yaw and CL at 20° outwards yaw (Figure 10

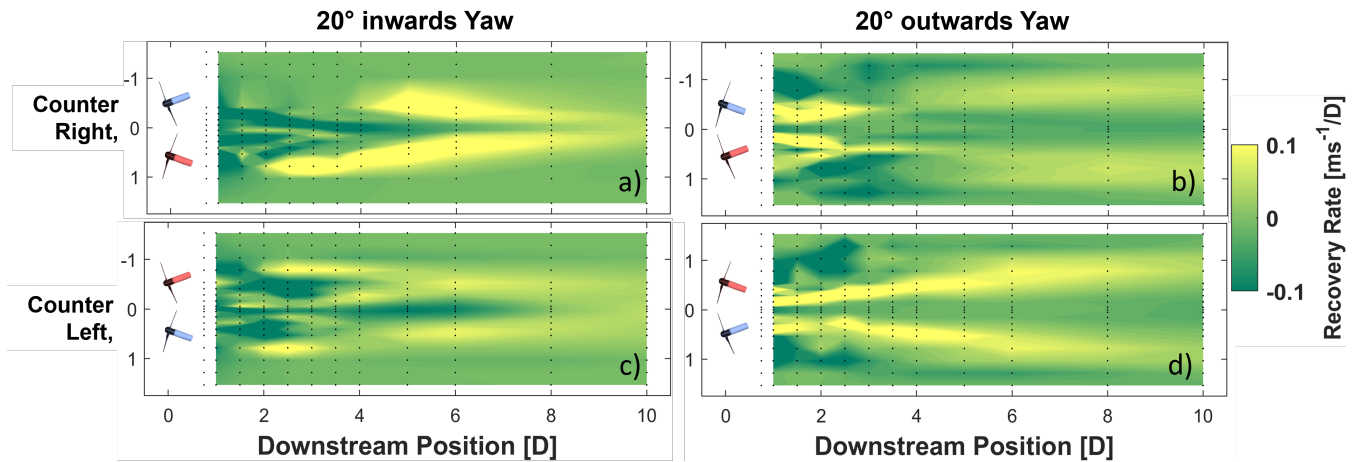


Figure 10. Streamwise recovery rate of both rotor configurations at 20° inwards (a and c) and 20° outwards (b and d) yaw. Counter-clockwise rotating turbine in red and clockwise rotating turbine in blue. Actual wake recovery dyed yellow and wake buildup colored in dark green.

a and d). Due to a strong wake-deflection either into (CR, 20° inwards) or away from each other (CL, 20° outwards), the flow downwind of the dual rotor is able to recover quickly, with highest recovery rates between approx. 2.5-6 D. This makes its application highly appealing for use in wind farms, where numerous turbines are positioned closely together and rapid flow recovery is essential.

250 When coupling the recovery rate to the rotational direction of the rotor, a faster recovery is always found on that side of the turbine, where the blades move in an upward direction. As the wake is rotating in the opposite direction as the rotor, this finding proves the relevance of flow entrainment from above the turbines for the wake recovery. As the wake is rotating in a downward direction, the flow from above the turbine is pulled into the measurement plane, accelerating the recovery of the wake.

In order to quantify the benefit on wake recovery through yaw misalignment, Equation 4 has been introduced. It integrates
255 the wind velocity over the span of the dual rotor and relates it to the reference inflow wind speed. Instead of showing the spacial distribution and explaining different mechanisms or wake-artefacts, this method allows a comparison of all investigated rotational and yaw-cases in one graph. It summarizes the quality of the dual-rotor wake recovery and quantifies how much relative wind a turbine, positioned downwind of the first turbine, has available. To do this, the the integration boundaries are set to -1.035 - 1.035 D, which corresponds to the span of the dual rotor.

260 Figure 11 shows the downstream evolution of the relative average wind velocity in the wake of the investigated dual rotor turbine for all different yaw configurations and both rotational settings. In these plots a value of $U_{Rel} = 1$ would correspond to a fully recovered flow and $U_{Rel} = 0$ would mean a stagnation of the flow.

The reference case (black dashed line) shows the relative wind in the wake of a dual rotor with 0° yaw of the single turbines. In both cases (CR and CL), the relative wind speed drops until a few D downstream, followed by its recovery. This behaviour,
265 as mentioned earlier, is explained by the time it takes the pressure difference to balance between the surrounding flow and the near wake of each rotor (Boudreau and Dumas (2017); Sanderse (2009)). After the pressure gradient has been overcome,

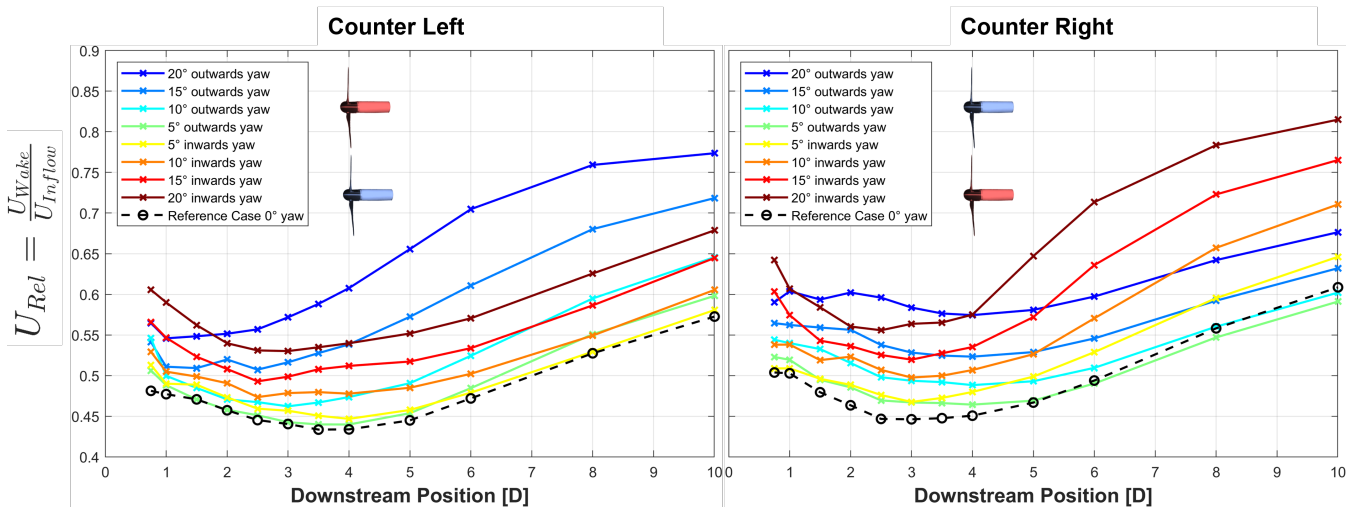


Figure 11. Line plots of the wind in the wake of a dual rotor, relative to the inflow. A value of $U_{Rel} = 1$ would correspond to a fully recovered velocity deficit.

energy is entrained from the surrounding flow through turbulent mixing and the wakes start to recover, resulting in an upward trend of the line in Figure 11.

Both in CL and in CR nearly all investigated cases follow the previously described principle, only that in some setups, the recovery either starts earlier or is generally better than in the reference case. Taking a closer look to the CL setup in Figure 11, one can observe that the point where the wake starts to recover (i.e. the lowest point of the curve) moves closer to the turbine, as the yaw misalignment is increased. The most extreme example is the relative windspeed in the wake in a 20° outwards yaw (Figure 11 left, dark blue line), which only drops until 1 D downstream and immediately starts to increase afterwards. This curve is marked not only by one of the earliest starts, but also by one of the fastest rates of recovery, reflected by the slope of the curve. Both factors result in the best relative windspeed in the CL setup at 10 D downstream, of more than 0.75.

For the CR setup (Figure 11 right), the earliest start of wake recovery and the fastest recovery rate, is seen in the 20° inwards yaw, with a relative windspeed of more than 0.8 at the end of the measurement plane (10 D). Even though the outwards yaw yields an overall faster relative flow at 10 D than the reference case, the start of the recovery is delayed until 4-5 D and the rate of recovery is moderate.

The difference in the recovery of the relative windspeed behind the different setups needs to be discussed separately between CR and CL. The earliest start of wake recovery for CR is found at the inwards yaw, hence directing the wakes into each other. In other studies it has already been found, that tip-vortex instability is of greatest relevance for the recovery of a wake (Lignarolo et al. (2014)). As the forced trajectory of the wakes trigger a quick collision and thus enhance the tip-vortex instability around a wake, a faster energy flux from the surrounding flow into the near wake is enabled and a quicker recovery can be seen.

For the CL outwards setup it is useful to look at the findings of the single wake deflection (subsection 3.1). It was found that the wake of a rotating turbine is deflected easier to the side, where the blades rotate in a downwards motion and recovers



better on the side with blades in upward motion. For the CL setup, this is the case on the inside, along the centerline of the setup. Following, the individual wakes are directed strongly away from each other causing the flow above the turbines to fill the low-pressure field in between the turbines and hence resulting in the highest relative windspeed downstream of the turbines and the fastest wake recovery.

In summary, nearly all yawed configurations yielded a better flow recovery than a dual rotor without yaw. This can be explained by either having a much quicker wake recovery caused by self-induced tip-vortex instability through wake collision; or by directing the trajectory of the wakes away from a possible downwind turbine and accelerating the entrainment from above.

4 Conclusions

This study presents an experimental approach to characterize the wake evolution and interaction behind a dual rotor turbine with counterrotating rotors in dependency of the respective yaw. In order to achieve that, two MoWiTO 0.6 were positioned in a wind tunnel at a lateral hub-hub distance of 1.07 D. Their yaw was alternated between a mirror symmetrical outwards and inwards yaw of 20° at a step size of 5°, so that in total 9 different yaw-setups were investigated per each of the two rotational cases (CR and CL). The wake was monitored through a hot-wire array, which traversed between 0.75 - 10 D behind the turbines.

In order to have a baseline behavior of the individual rotors, both the wake of the clockwise and counterclockwise rotating turbine were investigated individually in dependency of their yaw. In these preceding experiments it was already observed that the wake steering of a turbine is greatly dependent on the rotational sense of the setup. It was found that a wake is much easier deflected to the side, where blades move in a downward direction and the wake, as its rotating in the opposite direction of the blades, in upward direction. For the clockwise rotating case, this means a deflection to the right is enhanced, and vice versa for a counterclockwise rotating individual turbine.

After arranging the turbines in the dual rotor configuration, this effect could be transferred to the two different rotational configurations. It was easier to deflect the rotor wakes towards the centerline, when the clockwise rotating turbine was positioned left. The strongest split of the individual rotor wake was achieved by operating the clockwise rotating turbine on the right. The underlying mechanism for that was found to be the rotating wake interacting with the tower wake on the one side, and the free undisturbed flow on the other side. It is suggested that the tower wake, when drawn into the measurement plane, decelerates and widens the wake, while on the other side an entrainment of free undisturbed flow from above the rotor accelerates the recovery.

These findings are supported by the profiles of turbulent kinetic energy, where, under the concept of added turbulence, those regions of the wakes show the strongest fluctuations, where the tower wake gets drawn into the measurement plane. It was shown that when yawed inwards the colliding tip vortices of both rotor wakes in combination with the tower wakes generate an extremely turbulent field along the centerline, followed by a quick wake recovery.

Finally an analysis of the relative wind velocity in the wake showed that almost all rotational and yaw configurations yielded a better recovery of the wake than the reference case of 0° yaw. The two predominant factors for that were found to either



320 be the outwards centroid deflection, away from a possible downwind turbine or a faster interaction of the turbulent wakes. As found in literature (Lignarolo et al. (2015)) the tip vortex stability plays a fundamental role in the decay and recovery of a wind turbine wake. Hence, the direction of two wakes into each other triggers an accelerated vortex breakdown and contributes to a faster recovery.

For a future possible implementation of dual rotors in a windpark, these findings demonstrated possible gains for the turbines
325 in second or third row. The ease of directing the wakes either apart, for an enhanced flow entrainment from above, or into each other, to target tip vortex instability, are two possible paths to increase the overall power output of the wind farm. As it was found that the lateral interaction of wakes is a complex three dimensional mechanism, vertical investigations of the setup at hand shall clarify, in how far the concepts can be applied below or above hub height.

330 *Data availability.* The data that support the findings of this study are available in the data repository of Maus (2026).

Author contributions. In the scientific process, JM developed the methodology in close contact with MH. The investigation, formal analysis, visualization as well as writing the original draft was performed by JM. The initial concept, resources, supervision and the project administration was provided through MH, as well reviewing and curating the paper drafts. JP contributed in a supervising role.

Competing interests. At least one of the (co-)authors is a member of the editorial board of Wind Energy Science.

335 *Acknowledgements.* The author would like to thank all colleagues of ForWind, University of Oldenburg, for helping hands, fruitful discussions and assistance during and after the measurements. We would like to especially thank Julian Jüchter for the development and help with the MoWiTO 0.6.



References

- Bastankhah, M. and Porté-Agel, F.: Wind farm power optimization via yaw angle control: A wind tunnel study, *Journal of Renewable and Sustainable Energy*, 11, <https://doi.org/10.1063/1.5077038>, 2019.
- Boudreau, M. and Dumas, G.: Comparison of the wake recovery of the axial-flow and cross-flow turbine concepts, *Journal of Wind Engineering and Industrial Aerodynamics*, 165, 137–152, <https://doi.org/10.1016/j.jweia.2017.03.010>, 2017.
- Chasapogiannis, P., Prospathopoulos, J. M., Voutsinas, S. G., and Chaviaropoulos, T. K.: Analysis of the aerodynamic performance of the multi-rotor concept, *Journal of Physics: Conference Series*, 524, 012 084, <https://doi.org/10.1088/1742-6596/524/1/012084>, 2014.
- 345 Cherubini, S., Cillis, G. D., Semeraro, O., Leonardi, S., and Palma, P. D.: How incoming turbulence affects wake recovery of an NREL-5MW wind turbine, *Journal of Physics: Conference Series*, 2385, 012 139, <https://doi.org/10.1088/1742-6596/2385/1/012139>, 2022.
- EnBW and Aerodyn: Floating wind turbine: Nezy², <https://www.enbw.com/renewable-energy/wind-energy/our-offshore-wind-farms/nezy2-floating-wind-turbine/>, 2021.
- Ge, M. and Friedrich, J.: Greenhouse Gas Emissions by Countries and Sectors, <https://www.wri.org/blog/2020/02/greenhouse-gas-emissions-by-country-sector>, 2020.
- 350 Ghaisas, N., Ghate, A., and Lele, S.: Effect of tip spacing, thrust coefficient and turbine spacing in multi-rotor wind turbines and farms, *Wind Energy Science*, 5, 51–72, <https://doi.org/10.5194/wes-5-51-2020>, 2020.
- Howland, M. F., Bossuyt, J., Martínez-Tossas, L. A., Meyers, J., and Meneveau, C.: Wake structure in actuator disk models of wind turbines in yaw under uniform inflow conditions, *Journal of Renewable and Sustainable Energy*, 8, 4, <https://doi.org/10.1063/1.4955091>, 2016.
- 355 Jiménez, Á., Crespo, A., and Migoya, E.: Application of a LES technique to characterize the wake deflection of a wind turbine in yaw, *Wind Energy*, 13, 559–572, <https://doi.org/10.1002/WE.380>, 2010.
- Lignarolo, L. E., Ragni, D., Krishnaswami, C., Chen, Q., Simão Ferreira, C. J., and van Bussel, G. J.: Experimental analysis of the wake of a horizontal-axis wind-turbine model, *Renewable Energy*, 70, 31–46, <https://doi.org/10.1016/j.renene.2014.01.020>, 2014.
- Lignarolo, L. E., Ragni, D., Scarano, F., Simão Ferreira, C. J., and Van Bussel, G. J.: Tip-vortex instability and turbulent mixing in wind-turbine wakes, *Journal of Fluid Mechanics*, 781, 467–493, <https://doi.org/10.1017/jfm.2015.470>, 2015.
- 360 Maus, J.: Tip-Vortex Slow Motion - Model Wind Turbine Oldenburg, https://www.youtube.com/shorts/tMZ9C_ui_bQ, 2022.
- Maus, J.: Wake Interactions in a Counterrotating Dual Rotor System: Experimental HW-Measurements, <https://doi.org/10.57782/DNWQIO>, 2026.
- Maus, J., Peinke, J., and Hölling, M.: Experimental Investigation on the Effect of Lateral Turbine Spacing on Interactions of Wakes, *Journal of Physics: Conference Series*, 2265, 042 064, <https://doi.org/10.1088/1742-6596/2265/4/042064>, 2022.
- 365 Memija, A.: China's Mingyang Unveils Plans for Massive 50 MW Floating Wind Turbine, <https://www.offshorewind.biz/2025/10/21/chinas-mingyang-unveils-plans-for-massive-50-mw-floating-wind-turbine/>, 2025.
- Mendoza, V., Katsidoniotaki, E., Florentiades, M., Dot Fraga, J., and Dyachuk, E.: Aerodynamic performance of a dual turbine concept characterized by a relatively close distance between rotors, *Wind Energy*, 26, 521–537, <https://doi.org/10.1002/we.2813>, 2023.
- 370 Messmer, T., Brigden, C., Peinke, J., and Hölling, M.: A six degree-of-freedom set-up for wind tunnel testing of floating wind turbines, TORQUE 2022) *Journal of Physics: Conference Series*, 2265, 42 015, <https://doi.org/10.1088/1742-6596/2265/4/042015>, 2022.
- Neunaber, I.: Stochastic investigation of the evolution of small-scale turbulence in the wake of a wind turbine exposed to different inflow conditions, Dissertation, University of Oldenburg, 2019.



- Neunaber, I., Hölling, M., Stevens, R. J., Schepers, G., and Peinke, J.: Distinct turbulent regions in the wake of a wind turbine and their
375 inflow-dependent locations: The creation of a wake map, *Energies*, 13, 5392, <https://doi.org/10.3390/en13205392>, 2020.
- Newell, R. G., Raimi, D., and Aldana, G.: *Global Energy Outlook 2019: The Next Generation of Energy, Resources for the future*, p. 46,
www.rff.org/geo, 2019.
- Porté-Agel, F., Bastankhah, M., and Shamsoddin, S.: *Wind-Turbine and Wind-Farm Flows: A Review*, vol. 174, Springer Netherlands, ISBN
1054601900473, <https://doi.org/10.1007/s10546-019-00473-0>, 2020.
- 380 Sanderse, B.: *Aerodynamics of wind turbine wakes: Literature review*, Energy research Centre of the Netherlands, pp. 1–46,
<https://doi.org/10.1002/we>, 2009.
- Sandhu, N. S. and Chanana, S.: Performance and Economic Analysis of Multi-Rotor Wind Turbine, *EMITTER International Journal of
Engineering Technology*, 6, 289–316, <https://doi.org/10.24003/emitter.v6i2.298>, 2018.
- Schottler, J.: *Experimental Investigation of Wind Farm Effects using Model Wind Turbines*, Dissertation, University of Oldenburg, 2018.
- 385 Schottler, J., Hölling, A., Peinke, J., and Hölling, M.: Design and implementation of a controllable model wind turbine for experimental
studies, *Journal of Physics: Conference Series*, 753, <https://doi.org/10.1088/1742-6596/753/7/072030>, 2016.
- Schottler, J., Bartl, J., Mühle, F., Sætran, L., Peinke, J., and Hölling, M.: Wind tunnel experiments on wind turbine wakes in yaw: Redefining
the wake width, *Wind Energy Science*, 3, 257–273, <https://doi.org/10.5194/WES-3-257-2018>, 2018.
- Speakman, G. A., Abkar, M., Martínez-Tossas, L. A., and Bastankhah, M.: Wake steering of multirotor wind turbines: a new wind farm
390 control strategy, *Physics of Fluids*, pp. 1–20, <https://doi.org/10.1002/we.2633>, 2021.
- Van Der Laan, M. P. and Abkar, M.: Improved energy production of multi-rotor wind farms, *Journal of Physics: Conference Series*, 1256,
012011, <https://doi.org/10.1088/1742-6596/1256/1/012011>, 2019.
- Wu, Y. T. and Porté-Agel, F.: Large-Eddy Simulation of Wind-Turbine Wakes: Evaluation of Turbine Parametrisations, *Boundary-Layer
Meteorology*, 138, 345–366, <https://doi.org/10.1007/s10546-010-9569-x>, 2011.